Bryn Mawr College
Scholarship, Research, and Creative Work at Bryn Mawr College

Physics Faculty Research and Scholarship | Physics

2015

Methoxy and Methyl Group Rotation: Solid State NMR 1H Spin-lattice Relaxation, Electronic Structure Calculations, Xray Diffractometry, and Scanning Electron Microscopy

Peter A. Beckmann
Bryn Mawr College, pbeckman@brynmawr.edu

Clelia W. Mallory

Frank B. Mallory

Arnold L. Rheingold

Xianlong Wang

Let us know how access to this document benefits you.

Follow this and additional works at: http://repository.brynmawr.edu/physics_pubs


Part of the Physics Commons

Custom Citation

Beckmann P.A, Mallory C.W., Mallory F.B., Rheingold A.L., Wang X. "Methoxy and Methyl Group Rotation: Solid-State NMR (1) H Spin-Lattice Relaxation, Electronic Structure Calculations, X-ray Diffractometry, and Scanning Electron Microscopy." Chemphyschem 16.7 (2015):1509-19.

This paper is posted at Scholarship, Research, and Creative Work at Bryn Mawr College. http://repository.brynmawr.edu/physics_pubs/99

For more information, please contact repository@brynmawr.edu.

Methoxy and Methyl Group Rotation: Solid State NMR ^{1}H Spin-lattice Relaxation, Electronic Structure Calculations, X-ray Diffractometry, and Scanning Electron Microscopy

Peter A. Beckmann,[*] [a] Clelia W. Mallory,[b] Frank B. Mallory,[c] Arnold L. Rheingold,[d] and Xianlong Wang[*] [e]

[a] *Prof. P. A. Beckmann*
Department of Physics
Bryn Mawr College
Bryn Mawr, Pennsylvania, USA
Email: pbeckman@brynmawr.edu

[b] *Dr. C. W. Mallory*
Department of Chemistry
University of Pennsylvania
Philadelphia, Pennsylvania, USA

[c] *Prof. F. B. Mallory*
Department of Chemistry
Bryn Mawr College
Bryn Mawr, Pennsylvania, USA

[d] *Prof. A. L Rheingold*
Department of Chemistry and Biochemistry
University of California, San Diego
La Jolla, California, USA

[e] *Dr. X. Wang*
Key Laboratory for NeuroInformation of Ministry of Education
School of Life Science and Technology
University of Electronic Science and Technology
Chengdu, China
Email: wangxianlong@uestc.edu.cn

key words: density functional theory calculations; molecular dynamics; solid state NMR relaxation; x-ray diffraction; methyl group rotation.

ChemPhysChem 2015 16 1509-1519

ABSTRACT

We report solid state ^{1}H nuclear magnetic resonance (NMR) spin-lattice relaxation experiments, X-ray diffractometry, field emission scanning electron microscopy, and both single molecule and cluster *ab initio* electronic structure calculations in 1-methoxyphenanthrene (**1**) and in 3-methoxyphenanthrene (**2**) to investigate the rotation of the methoxy groups and their constituent methyl groups. The electronic structure calculations and the ^{1}H NMR relaxation measurements can be used together to determine barriers for the rotation of a methoxy group and its constituent methyl group and to develop models for the two coupled motions.

INTRODUCTION

For some time we have been engaged in an ongoing investigation of methyl group rotation in aromatic organic compounds in the crystalline state for the case where the methyl group is bonded directly to a rigid backbone.[1-3] In this case, at higher temperatures, thermally activated methyl group rotation[4] is the only motion on the nuclear magnetic resonance (NMR) time scale (10^{-5} to 10^{-12} s in our case). The goal is to relate structure (molecular and crystal) and dynamics and the experimental tools are solid state NMR ^{1}H and ^{19}F spin-lattice relaxation,[5] X-ray diffraction,[6] field emission scanning electron microscopy (FESEM)[7] and the computational tool is ab initio electronic structure calculations,[8] both in the isolated molecules and in a central target molecule in clusters of molecules constructed from the X-ray diffraction data. The calculated methyl group barriers can be compared with, and related to,[9, 10] the activation energies determined from the solid state NMR experiments. The FESEM images aid in the interpretation of the solid state NMR experiments. This work and our more recent studies[11-13] have extended this investigation to compounds with methoxy groups attached to an aromatic ring rather than just methyl groups attached directly to an aromatic ring.[3] This allows for an additional degree of freedom (methoxy group rotation or libration in addition to the rotation of the methoxy group's constituent methyl group) and has allowed us to extend and test our models for methyl group rotation.

NMR, coupled with other experimental and computational techniques can be used to investigate the motion of a variety of molecular and intramolecular moieties in the solid

state.[14-21] ^{1}H NMR spectroscopy,[20] ^{2}H NMR spectroscopy,[14, 15, 19, 21] ^{13}C NMR spectroscopy,[16-19] ^{31}P NMR spectroscopy,[16] and ^{1}H NMR relaxation[1-3, 11-13, 17] have all been used in a variety of studies to investigate a wide variety of intramolecular motions[1-3, 11-20] and motions of guests in inclusion compounds.[21] One study has investigated methoxy and methyl group dynamics (as well as the motion of other moieties) in a very complicated system using ^{13}C NMR spectroscopy[17] but we are unaware of any studies other than ours[11-13] that have investigated and carefully modeled the coupled rotation of a methoxy group and its constituent methyl group using nuclear spin relaxation techniques.

Here, we use 1-methoxyphenanthrene (**1**) and 3-methoxyphenanthrene (**2**) (Fig. 1) to extend and further clarify the coupled motion of a methoxy group and its constituent methyl group, including both barriers for rotation *and* the timescales of the motions involved. We compare the results in **1** and **2** with the previous studies with 4,4'-dimethoxybiphenyl[12, 13] (**3**) and with 4,4'-dimethoxyoctafluorobiphenyl[11] (**4**) (Fig. 1) in which significant complications resulting from the degree of freedom for the relative orientation of the two phenyl groups were discussed.

RESULTS

X-ray Diffraction

Small crystals of **1** and **2** were taken from the same samples used to perform the NMR relaxation experiments. The details of the structures are given in Table 1. For comparison, Table 1 also includes the previously published structural information for **3**[12] and **4**.[11] The crystal structures for **1** and **2** are shown in Figs. 2 and 3 where the number of molecules shown corresponds to the clusters used in the electronic structure calculations as discussed below. The important feature of the structures both for the interpretation of the NMR relaxation experiments and the electronic structure calculations (both discussed below) is that the asymmetric unit (*Z*' in Table 1) is a single molecule in both **1** and **2** which means all methoxy groups (along with their constituent methyl groups) are equivalent.

Scanning Electron Microscopy

Figs. 4 and 5 show field emission scanning electron microscopy[7] images of (small parts of) the same polycrystalline samples of **1** and **2** used in the solid state NMR ^{1}H spin-lattice relaxation experiments. The crystallites in **1** (Fig. 4) are long with approximately square cross sections. The smallest dimensions of the majority of the crystallites are 15-40 μm and they appear to be single crystals in that the crystals are smooth on the 100s nm scale. If this is the case, the fraction of molecules near a surface is completely negligible. The crystallites of **2** are flat plates and their smallest dimension is not clear. The flake shown in Fig. 5 is a typical one and is very large in two dimensions; approximately 0.5 mm X 0.5 mm. Even if this corresponds to a single crystal in two dimensions, an important question is, how large is the third dimension? The white box in Fig. 5a is in a region that appears to be a break in this flake. The increased magnification in Figs. 5b and 5c shows possible structure in the approximately 10 μm thickness of the flake. If this is just a "rough edge" of a single crystal, then the smallest dimension is approximately 10 μm in which case the number of molecules near a surface is negligible.[2] However, this rough edge may indicate either that there are very thin single crystals stacked on top of one another or that there are many dislocations in the crystallite.

NMR Relaxation

For the random isotropic motion of the direction of the vector $\vec{r}$ between two spin-1/2 particles having a fixed distance *r* between them in a random distribution of such isolated (non-interacting) pairs, the ^{1}H nuclear spin-lattice relaxation is strictly exponential and the relaxation rate *R* (the inverse of the spin-lattice relaxation time T_1) is given by[2, 22] $R = A[J(\omega_N,\tau) + 4J(2\omega_N,\tau)]$ with $J(\omega,\tau) = 2\tau/(1 + \omega^2\tau^2)$ and $\tau = \tau_0[\exp(E/kT)]$. An additional assumption is that the motions of the (isolated) $\vec{r}$ vectors in the ensemble are uncorrelated. Here, *A* is a constant,[1] proportional to r^{-6}, that characterizes the (single) spin-spin dipolar interaction, $J(\omega,\tau)$ is the spectral density that characterizes the frequency distribution of the local time-dependent magnetic fields resulting from the motion of the spins, ω is an angular frequency, ω_N is the NMR angular frequency, τ is a mean time between hops from one position to another (of $\vec{r}$) in a random (Poisson) hopping model, τ_0

is a preexponential factor, and *E* is the NMR activation energy that can be compared with the calculated values of the barrier heights which are discussed below.

The following discussion assmes that in **1** and **2** the methoxy group's constituent methyl group is rotating on the NMR time scale and that the methoxy group is not. A methyl group involves three $\vec{r}$ vectors discussed in the previous paragraph and the hopping motion, though random, is not isotropic (all three $\vec{r}$ vectors orient in a plane) and the motion of the three $\vec{r}$ vectors is perfectly correlated. As such, as discussed extensively long ago,[23, 24] in this case the relaxation is nonexponential although in a polycrystalline sample (i.e., a random distribution of methyl group rotation axes) this nonexponential relaxation is only observed in the fast-motion limit ($\omega\tau << 1$; higher temperatures) and in the vicinity of the relaxation rate maximum ($\omega\tau \approx 1$).[23, 24] One of the several goals of this study is to adequately fit the decay of the ^{1}H magnetization following a perturbation-measure pulse sequence and properly extract the rate that should be used in applying the theory presented above when the relaxation is a consequence of the dipolar interactions (among the three ^{1}H spins in a methyl group) being modulated by methyl group rotation. In this study, the decay of the perturbed ^{1}H nuclear magnetization $M(t)$ was always fitted to both an exponential $\Delta M(t) = [\Delta M(0)]\exp(-Rt)$ and to a stretched exponential $\Delta M(t) = [\Delta M(0)]\exp\{-(R^*t)^{\beta}\}$. Here, $\Delta M(t) = M(\infty) - M(t)$ where $M(\infty)$ is the equilibrium ^{1}H nuclear magnetization and $M(0)$ is the magnetization immediately following the perturbation. R^* is the *characteristic* relaxation rate and $\beta < 1$ is the *stretching parameter* in the stretched exponential function. When $\beta = 1$, $R^* = R$. We have provided a review of the use of the stretched exponential in a wide variety of research areas.[13] As far as we know, neither R^* or β is amenable to any consistent theoretical interpretation involving methyl group rotation in these kinds of organic solids. The stretched exponential is simply a convenient way to characterize the degree of nonexponential relaxation involving only one parameter in addition to those required for exponential relaxation.

The model that predicts the nonexponential relaxation resulting from the modulation of the dipolar interactions which, in turn, result from the rotation of a methyl group,[23, 24] predicts that the initial recovery of the perturbed magnetization approaches a constant; that is $[\{d(\Delta M(t))/dt\}/\Delta M(0)]_{\lim t \to 0} = -R_S$ (which defines R_S where S means 'short time') whereas

the stretched exponential model predicts that $[\{d(\Delta M(t))/dt\}/\Delta M(0)]_{\lim t \to 0} \rightarrow -\infty$ for $\beta < 1$. As such, the stretched exponential is unphysical as $t \rightarrow 0$. In practice, NMR relaxation data of this kind never gets close enough to $t = 0$ for this unphysical feature to prevent the stretched exponential from fitting the data. Indeed, when the relaxation is nonexponential, the stretched exponential function fits the data very well. This, in and of itself, is an interesting observation, especially when one notes that the stretched exponential requires only one more fitting parameter than exponential relaxation. (Relaxation via a double exponential, for example, requires two additional fitting parameters.[13]) We are able to determine an initial decay rate R_S from the raw data in the manner outlined in detail elsewhere.[13] As such, *the stretched exponential function is simply an indicator of the degree of the nonexponential relaxation and plays no role in the final data analysis*. In this case R_S, the rate characterizing the initial relaxation of the nonexponential relaxation corresponds to the model above[23, 24] with $A = (n/N)C$.[1, 2] The parameter $n = 3$ is the number of ^{1}H spins in a methyl group and $N = 12$ (for both **1** and **2**) is the number of ^{1}H spins in the molecule. When $\omega\tau >> 1$ ('low' temperature), the relaxation is exponential and the relaxation rate R corresponds to the model presented above.[23, 24] Or, to put it another way, at lower temperatures, $\beta \rightarrow 1$ and $R^* \rightarrow R = R_S$ and the effects of non-isotropic motion and the perfect correlation of the three $\vec{r}$ vectors plays no role.

The temperature dependence of the relaxation rates R, R^*, and R_S at NMR frequencies of $\omega_N/2\pi$ = 22.5 and 53.0 MHz are shown in Fig. 6 for **1** and Fig. 7 for **2**. R_S and R (the latter corresponding to where the relaxation is exponential so $R = R_S$) are shown by squares (53.0 MHz) and circles (22.5 MHz) in Figs. 6 and 7 and the rate R^* (where different than R_S) is shown by triangles (pointing up for 53.0 MHz and pointing down for 22.5 MHz).

When, given the presence of noise, is an observed relaxation curve deemed to be nonexponential? Examples of recovery curves similar to those observed here are provided elsewhere.[13] Fig. 8 shows the temperature dependence of the parameter β in the fitting equation $\Delta M(t) = [\Delta M(0)]\exp\{-(R^*t)^\beta\}$ at both NMR frequencies in **1**. (The same plot in **2** is very similar.) The two vertical lines (one for each NMR frequency) indicate, on decreasing temperature, where β becomes approximately 0.93 (the horizontal full line) from

below that value at higher temperatures. When β is, approximately, greater than this, the relaxation is *deemed* to be exponential (within experimental uncertainty) and below this is taken to be nonexponential. The vertical lines in Fig. 8 correspond to the temperature in Figs. 6 and 7 below which R_S and R are (within experimental uncertainty) indistinguishable.

The adjustable parameters in the expression for R or R_S, then, are E, C and τ_0 in R or $R_S = (n/N)C[J(\omega_N,\tau) + 4J(2\omega_N,\tau)]$ with $J(\omega,\tau) = 2\tau/(1 + \omega^2\tau^2)$ and $\tau = \tau_0[\exp(E/kT)]$. (We note that if the methoxy group is also reorienting on the NMR time scale, the required model is very much more complicated. As discussed below, these models are unnecessary.) It is convenient to introduce the parameter $x = C/C_M$; the ratio of the fitted C value to the value $C_M = (9/40)(\mu_o/4\pi)^2(\gamma^4\hbar^2/r^6)$ one would obtain by considering only intramethyl spin-spin interactions.[1] Here, μ_o is the magnetic constant, γ is the ^{1}H magnetogyric ratio, and r = 0.1785 nm is the average distance between ^{1}H spins in the methyl groups (in **1** and **2** as determined by the electronic structure calculations in a cluster as discussed below). We can also take $\tau_{m0} = (2\pi/3)(I/2E)^{1/2}$ or other values within a factor of 2 or so of this value as a benchmark[1, 4, 25] for τ_0 and use $y = \tau_0/\tau_{m0}$ as the fitting parameter. Here, I is the moment of inertia of a methyl group. If, say, y is more than one or two orders of magnitude different from unity, then the motion is unlikely to be methyl group rotation.

The data for **1** is fitted to this single Poisson model in Fig. 6. Here, E = 16 ± 2 kJ mol^{-1} (Table 2), x = 1.1 ± 0.1, and y = 0.5 ± 0.3. The uncertainties are quite large because of the difficulty of measuring R_S accurately[13] at higher temperatures and because of the scatter in R at low temperatures, presumably resulting from small differences in packing at low temperatures as a consequence of different thermal histories. The uncertainties in $y = \tau_0/\tau_{m0}$ are always large because τ_0 multiplies an exponential function in $\tau = \tau_0[\exp(E/kT)]$ whose argument E itself has an uncertainty.

The data for **2** cannot be fitted to the single-site Poisson model presented above. We fit the data with a Davidson-Cole spectral density[2, 26, 27] $J(\omega,\tau) = [2/\omega][\sin\{\varepsilon \arctan(\omega\tau_{DC})\}]/[(1 + \omega^2\tau_{DC}^2)^{\varepsilon/2}]$ with $\tau_{DC} = \tau_{0DC}[\exp(E_{DC}/kT)]$[2] corresponding to a continuous distribution of E values between 0 and E_{DC} with E_{DC} being an upper limit cutoff corresponding to the perfect crystal value.[2] This model adds the additional parameter ε

to the Poisson model with $\varepsilon < 1$ and where $\varepsilon = 1$ corresponds to the Poisson model. That is, as $\varepsilon \rightarrow 1$, $[2/\omega][\sin\{\varepsilon \arctan(\omega\tau_{DC})\}]/[(1 + \omega^2\tau_{DC}^2)^{\varepsilon/2}] \rightarrow 2\tau/(1 + \omega^2\tau^2)$ with $\tau = \tau_{DC}$. The data for **2** is fitted to this Davidson-Cole model in Fig. 7 with E_{DC} = 16 ± 2 kJ mol^{-1} (Table 2), ε = 0.78 ± 0.08, x = 1.3 ± 0.1, and y = $0.2^{+0.2}_{-0.1}$. The great appeal of the Davidson-Cole model is that it introduces only one additional adjustable parameter, ε, making this a four-parameter fit. In the distribution of E values, E_{DC} is the upper limit cutoff and for ε = 0.78, the distribution is very sharply peaked at E_{DC}.[2] As such, it is both reasonable and appropriate to refer to E_{DC} as "the" methyl group activation energy.

The situation in **1** is the ideal case. All methyl groups (molecules) are equivalent. The NMR E = 16 ± 2 kJ mol^{-1} agrees with the value 16 kJ mol^{-1} computed using the electronic structure calculations (presented below), the value of $x \approx 1$ suggests that intramethyl group spin-spin interactions dominate, and the value of y ≈ 0.5 suggests that it is indeed an entity with the moment of inertia of a methyl group (or thereabouts) whose motion is responsible for the spin-lattice relaxation. The SEM images (Fig. 4) support this interpretation; the crystallites are large and the fraction of methyl groups that might have a different rotational barrier because they are near a surface is completely negligible.

The situation in **2** is somewhat problematic (though internally consistent). The SEM images (Fig. 5) are difficult to interpret but one possible interpretation is that the crystallites may be very thin (or they may have many discontinuities) and that there may be an appreciable number of methyl rotors near a surface (or some other crystal imperfection). This would indeed lead to a situation where the Poisson spectral density is not appropriate and where the Davidson-Cole spectral density might be a first crude attempt at quantifying the distribution in methyl group activation energies.[2] E_{DC} = 16 ± 2 kJ mol^{-1} is not so different from the calculated value of 13 kJ mol^{-1} (presented below). More troubling is that $x = C/C_M$ = 1.3 ± 0.1 which is significantly greater than unity. This suggests that methyl group – nonmethyl group ^{1}H spin-spin interactions are contributing significantly to the relaxation. A careful investigation of methyl group H – nonmethyl group H (either intramolecular or intermolecular) distances using the crystal structure (Fig. 3) suggests that this is not the case. We are investigating this phenomenon further in a variety of experiments.

Electronic Structure Calculations

Isolated Molecules

There are two kinds of internal rotational degrees of freedom in **1** and **2**: methoxy group rotation around the O-C*n* bond (*n* = 1 in **1** and *n* = 3 in **2**) (see Fig. 1) and methyl group rotation around the Cm-O bond. Here, Cm refers to the methyl carbon atom. Dihedral angles δ (Cm-O-C1-C2) and α (H-Cm-O-C1) in **1** and dihedral angles δ (Cm-O-C3-C4) and α (H-Cm-O-C3) in **2** are used as the rotational coordinates of the methoxy group and the methyl group, respectively. The methoxy groups in **1** and **2** have a different intramolecular environment. In **1**, the H atom at the 10-position provides a gatekeeper role to the rotation of the 1-methoxy group while there is no such steric hindrance in **2**. The calculated isolated molecule structures of **1** and **2** are similar to the structures of the molecules in the crystal as determined by X-ray diffraction. The electronic structure calculations for an isolated molecule reproduce the bond lengths, bond angles, and most bond dihedral angles found in the molecule in the crystal. The greatest difference lies in the dihedral angles δ formed between the 4-methoxy group and the phenanthrene ring. In the ground state of an isolated molecule of **1**, the Cm-O bond is coplanar with the ring on the C1-C2 side (δ = 0°) as shown in Fig. 1 whereas in the crystal, δ = 4.3°. In the ground state of an isolated molecule of **2**, the Cm-O bond is coplanar with the ring on the C3-C4 side (δ = 0°) whereas in the crystal, δ = 8.5°. These differences in δ between the isolated molecules and the molecules in the crystal reflect the competition between non-bonded intramolecular interactions and intermolecular interactions in the crystal packing environment.

The potential energy surfaces (PESs) for the coupled internal rotations of the methoxy group and its constituent methyl group in **1** and **2** are shown in Figs. 9a and 9b. The methoxy group angle δ is shown for $0^O < \delta < 180^O$ and the methyl group angle α is shown for $0^O < \alpha < 60^O$. The plots for $180^O < \delta < 360^O$ and the plots for $60^O < \alpha < 120^O = 0^O$ are mirror images of the plots shown.

In **1** (Fig. 9a) the short dashed lines show the coupled methoxy-methyl group journey from the methoxy-methyl group ground state (δ, α) = (0^O, 60^O) to the methoxy group transition state (δ, α) = (180^O, 58^O) and the long dashed lines show the coupled

methoxy-methyl group journey from the methoxy-methyl group ground state (δ, α) = (0^{O}, 60^{O}) to the methyl group transition state (δ, α) = (30^{O}, 0^{O}). Although the methyl group has approximately the same orientation in the methoxy group ground and transition states in **1**, it reorients considerably en route, with a maximum rotation of about $\alpha = 50^{O}$ (from 60^{O} to 10^{O}) when the methoxy group is approximately $\delta = 135^{O}$. This methyl group rotational response is due to strong steric interactions with the H atom in the 10 position. The methoxy group barrier is 40.5 kJ mol^{-1}, the methyl group barrier is 13.8 kJ mol^{-1}, and these values are reported in Table 2.

In **2** (Fig. 9b) the short dashed lines show the coupled methoxy-methyl group journey from the methoxy-methyl ground state (δ, α) = (0^{O}, 60^{O}) to the methoxy group transition state (δ, α) = (180^{O}, 60^{O}) and the long dashed lines show the coupled methoxy-methyl group journey from the methoxy-methyl group ground state (δ, α) = (0^{O}, 60^{O}) to the methyl group transition state (δ, α) = (27^{O}, 0^{O}). Here there is no steric interaction as in the case of **1** and the methyl group does not appreciably reorient as the methoxy group rotates from the ground state to the transition state. The methoxy group barrier is 13.7 kJ mol^{-1} (significantly less than in **1**), the methyl group barrier is 13.8 kJ mol^{-1} (the same is in **1**), and these values are reported in Table 2.

Clusters

Clusters of **1** and **2** were constructed from the single-crystal X-ray structures to mimic the intermolecular environment in the crystals. We have recently compared using clusters with using periodic boundary conditions.[28] A 10-molecule cluster and a 14-molecule cluster of **1** were constructed to examine the effect of cluster size on the calculated barriers and both are shown in Fig. 2. Only one cluster consisting of 12 molecules was built for **2** and it is shown in Fig. 3. The environment of the central molecule in each cluster simulates the crystal packing interactions as experienced by a molecule in an ideal crystal. For the first step [*the rigid rotation model* (see the Experiments section)], all C and O atoms were fixed at the positions determined in the X-ray structure but the positions of all H atoms in the clusters were determined by the calculations. This is important because the X-ray experiments position the H atoms (placed in idealized positions) with C–H bond lengths that are too short by approximately 0.10 Å.[29, 30]

Determining H atom positions accurately is important in interpreting the NMR relaxation measurements because the H–H distances in a methyl group *r* enter into the calculation of the NMR parameter $C_M = (9/40)(\mu_o/4\pi)^2(\gamma^4\hbar^2/r^6)$ as r^{-6} as discussed in the solid state NMR relaxation rate section above. As such, a given percent uncertainty or error in *r* results in six times that percent uncertainty or error in C_M.

One dimensional PESs were calculated for the internal rotations (methyl and methoxy) on the target molecule of each cluster. Several groups of calculations were performed as outlined in the Experiments section. Fig. 10 shows the PESs (calculated at the level of the *rigid rotation model*) of the methoxy group on the home molecule in the clusters for both **1** and **2** and Fig. 11 shows the PESs of the methoxy groups' constituent methyl groups. For the methoxy group in both compounds, we see that the barriers increase to more than 1000 kJ mol^{-1} in the clusters; this is not very surprising since the methoxy rotation is highly angularly anisotropic. The intermolecular interactions will quench rotations over the barrier in the crystal environment. On the basis of this *rigid rotation model* calculation we can say that if additional atoms in the cluster were relaxed (see the Experiments section) the barrier for methoxy group rotation would decrease, but not below a level that would allow rotation over the barrier. In Table 2, we indicate that the barrier > 800 kJ mol^{-1}. Yet, there is a flat bottom to the PES ($\delta = 0^O$ to 30^O in Fig. 10) around the ground state characterized by $\delta = 4.3^O$ in **1** and $\delta = 8.5^O$ in **2.** This suggests that the methoxy group will librate over a large range in the crystal (approximately $\delta = -30^O$ to $+30^O$). As seen in Fig. 11, for the more symmetric methoxy group's constituent methyl group, the rotational barrier calculated using the *rigid rotation model* increases from 13.8 kJ mol^{-1} in the isolated molecule to 25.2 kJ mol^{-1} in the clusters of both compounds. See also Table 3. The geometry of the ground state changes slightly in the clusters, the methyl group $\alpha = 67^O$ in **1** and $\alpha = 56^O$ in **2** compared with $\alpha = 60^O$ in the isolated molecules. The likely reason for this slight change is due to the off-plane orientation of the methoxy group in the crystal ($\delta = 4.3^O$ in **1** and $\delta = 8.5^O$ in **2**). The results calculated in both the 10 and 14-molecule clusters of **1** are almost identical for both the methoxy group and its constituent methyl group as indicated in Table 3. For example, the methyl rotational barrier calculated in the 10-molecule cluster is 25.5 kJ mol^{-}

[1], higher by only 0.3 kJ mol^{-1} than the barrier calculated in the 14-molecule cluster. These values are indicated in Table 3.

Methyl group rotation was further investigated by *partial relaxation models* in which intra- and intermolecular structural relaxation freedom was included at multiple stages in a sequential order as presented in the Experiments section. The barrier heights calculated at different partial relaxation stages and at different theoretical levels are tabulated in Table 3 with the "final" values also indicated in Table 2 where they can be compared with the activation energies determined from the ^1H spin-lattice relaxation measurements.

The most significant change in going from the *rigid rotation model* to the several stages of the *partial relaxation model* occurs at the first (*intramolecular relaxation*) stage where the structural parameters of the methoxy group and the H atoms on the home molecule were allowed to relax. There are no significant changes in the later *intermolecular relaxation* stages (see the Experiments section and Table 3) for both compounds. In **1**, the methyl group barrier height decreases from 25.2 kJ mol^{-1} in the *rigid rotation model* to 16.6 kJ mol^{-1} in the *partial relaxation mode*l using the 14-molecule cluster. In **2**, the barrier height decreases from 25.2 kJ mol^{-1} in the *rigid rotation model* to 13.4 kJ mol^{-1} in *the partial relaxation model*. These values are indicated in Table 3. The final values are similar to both the values for the rotational barrier in the isolated molecules and to the NMR activation energies (Table 2).

For both compounds in the solid state, the structural relaxation of the methoxy group, particularly the changes in the dihedral angles, is the main cause for the decrease of the methyl group barriers in going from the *rigid* to the *partially relaxed* computational models. In **1** the methoxy dihedral δ increases slightly from 5.4^O to 9.8^O as the methyl group changes from the ground state ($\alpha = 67^O$) to the transition state ($\alpha = 0^O$) This change in methoxy group orientation is indicated in Table 2, where the change can be compared both with the change in the isolated molecule and with the equivalent changes in the other compounds of interest in this study. Note that the dihedral angle in the optimized ground state for **1** is very close to the value found in the crystal, 4.3^O. The bond angle of Cm-O-C1 also increases by 3.6^O to 122.0^O in the transition state from 118.4^O (compared with 117.4^O in the crystal). In **2**, the *partially relaxed* ground state

structure is essentially the same as that found in the X-ray crystal structure. But in the methyl group rotational transition state, the methoxy group reorients by 7.8^{O} (δ changes from 8.5^{O} from the ground state to 16.2^{O} in the transition state), a similar change to that found in **1**. The bond angle of Cm-O-C3 also increases by 3.8^{O} to 121.1^{O} in the transition state from 117.3^{O} in the ground state. In both compounds, there is another kind of common intramolecular structural relaxation: the methyl group bond angles between the Cm-H bonds and the Cm-O bond increase or decrease by a few degrees. This structural relaxation is common for all methyl groups attached to aromatic rings since the rotation switches the in-plane and out-of-plane Cm-H bonds alternatively. Even though the phenanthrene ring of the home molecule in the clusters of **1** was also allowed to relax in the *stage four* of the *partial relaxation model* (see the Experiments section), there were no significant changes observed for the ring; neither did the methyl group barrier change. This again indicates that *stage one* of the *partial relaxation* scheme is a reasonable model and contains all the necessary relaxation possibilities.

In addition to using the B3LYP/6-31G(d) model,[31-33] we also checked how the inclusion of the basis state superposition error (BSSE) correction using the counter-poise algorithm[34, 35] and London's dispersion correction with the Grimme's D3 method,[36, 37] would affect the barrier. We also compared the barriers calculated at two other hybrid functionals, TPSSh[38] and M06-2X,[39] with the value calculated using the B3LYP functional. The comparative calculations were done on the *stage four* geometries (see the Experiments section) of the clusters of **1** and the results are given in Table 3. From the results, we see that the correction for the BSSE or for London's dispersion does not have a significant effect on the barriers. The TPSSh barrier also agrees well with the B3LYP barrier. The exception is that the M06-2X functional results in a higher methyl group barrier than the B3LYP functional by ~3.5 kJ/mol. The conclusion is that the theoretical model applied here [i.e., B3LYP/6-31G(d)] and in previous studies[2, 3, 11, 12, 28, 40] is reliable even without the corrections for the BSSE and London dispersion since the corrections change the barriers only slightly, in part because the changes for the two corrections are of the opposite sign. The exceptionally larger barrier obtained with the M06-2X functional is possibly due to the fact that the functional includes more Hartree-Fock exchange energy than the other two functionals. In previous studies,[40] we have

seen the Hartree-Fock model itself gives consistently higher barriers than the B3LYP model.

DISCUSSION AND CONCLUSIONS

We have performed X-ray diffractometry, solid state NMR ^{1}H spin-lattice relaxation, field effect scanning electron microscopy, and electronic structure calculations in 1-methoxyphenanthrene (**1**) and in 3-methoxyphenanthrene (**2**). Similar studies have been performed in 4,4-dimethoxybiphenyl[12, 13] (**3**) and in 4,4'-dimethoxyoctafluorobiphenyl[11] (**4**). The four molecules are shown in Fig. 1. In Table 1, we compare a variety of structural parameters in these four compounds determined by X-ray diffraction and in Table 2 we compare parameters characterizing methyl group and methoxy group rotation from both the electronic structure calculations (isolated molecules and crystals) and the solid state NMR ^{1}H spin-lattice relaxation measurements (solid state only). The significant differences in many of the entries in Table 2 for **4** (compared with the similarities among **1-3**) can be traced to the fact that whereas the methoxy groups in **1-3** all have neighboring H atoms on the ring, the methoxy groups in **4** have much larger neighboring F atoms on the ring.

The calculated barriers for rotation in the isolated molecules are labeled V_{iso} and the barriers in the clusters are labeled V_{clust} (Table 2). V_{clust} can be compared with V_{iso} to provide some idea of the relative role of intramolecular and intermolecular contributions to the barrier. For the methoxy group, $V_{clust} >> V_{iso}$ in all four compounds as a consequence of the role that the intermolecular interactions in the crystal have on such an asymmetric group. Indeed, methoxy group rotation over the barrier will be quenched in the solid state though there will be libration (oscillations) about the ground state rotational angle. For the rotation of the methoxy group's constituent methyl group, V_{clust} can be about the same (e.g., in **2**), somewhat less (e.g., in **3**), somewhat greater (e.g., in **1**), or much greater (e.g., in **4**), than V_{iso}. A barrier is a *difference* between the energy in the rotational ground state and the energy in the rotational transition state and intermolecular interactions can raise the two energies by different amounts. As such, the barrier can increase or decrease (or stay the same). Since intermolecular interactions in the crystal change the angles and bond lengths (from those found in the isolated molecules) that characterize the methoxy groups, a detailed specific distinction between intramolecular and intermolecular

interactions for methyl group rotation becomes somewhat ill defined since, in some sense, going from the isolated molecule to the solid state, intermolecular interactions change the intramolecular interactions. The fitted NMR activation energies E for methyl group rotation can be compared with the barriers V_{clust} determined using electronic structure calculations (Table 2).

The calculations that determine the barriers V_{clust} account for the coupled rotation of a methoxy group and its constituent methyl group. That is, in calculating the barrier for one, the other rotates in order for the system to achieve a minimum energy configuration. This coupled rotation for the isolated molecules is indicated in Fig. 9 for the molecules studied here. Constructing such a plot for the clusters (mimicking the solid state) is far beyond the computing power available to us. But we can say that the methoxy group barrier in the solid state is so large for **1**-**4** that there is no need to do this calculation; the methoxy group never achieves a departure from the ground state where there is appreciable methyl group rotation. The calculations indicate that in the solid state, as the methyl groups rotate approximately 60^{O} from the ground state to the transition state, the methoxy groups rotate (Table 2) 5^{O} (5^{O} from the ring to 10^{O} from the ring), 7^{O} (9^{O} to 16^{O}), 16^{O} (3^{O} to 19^{O}), and 29^{O} (13^{O} to 42^{O}) in **1**-**4**. The magnitudes of these rotations increase as the barrier for methoxy group rotation in the isolated molecules decreases (Table 2). Finally, we note that the electronic structure calculations by themselves say nothing about the times cales of these various rotations and librations; they just calculate an energy as a function of two rotational angles.

The temperature dependence of the solid state ^{1}H NMR spin-lattice relaxation can be fitted to determine several relevant parameters and it can contribute to the matter of the time scales of the various motions. In all four compounds **1**-**4**, the parameters related to the overall average strength of the dipolar ^{1}H spin – ^{1}H spin interactions and the preexponential factor in an Arrhenius relationship are *only* consistent with the motion (on the NMR time scale) being methyl group rotation only. They are *not* consistent with the spin-spin interaction being further modulated by methoxy group libration. This suggests that the methoxy group libration occurs on a time scale that is too fast to affect the NMR relaxation. The effect of this high frequency methoxy group libration in the NMR experiments is to add a time-dependent distribution of methyl group rotation axes to the

already present spatial distribution of methyl group rotation axes in the large (≈ 0.5 g) polycrystalline samples used in the NMR experiments.

In this study we have carefully investigated the nonexponential nature of the ^{1}H spin-lattice relaxation rate[23, 24] at two NMR frequencies and over a wide temperature range; wide enough to investigate both the long and short correlation time limits. When the mean frequency of methyl group hopping in a random (Poisson) process is small compared with the NMR frequency ('low' temperatures), the relaxation is observed to be exponential. When the mean frequency of methyl group hopping is large compared with the NMR frequency ('high' temperatures), the relaxation is observed to be nonexponential as predicted.[23, 24] Although the nonexponential relaxation is fitted very precisely by a stretched exponential function, this is of little consequence (other than to monitor the degree of nonexponentiality) since the parameters so obtained are not amenable to theoretical interpretation. In this case, the short time relaxation is amenable to theoretical interpretation.

EXPERIMENTS

Synthesis

1-Methoxyphenanthrene (**1**) was prepared by oxidative photocyclization of 2-methoxystilbene[41] in cyclohexane solution with iodine as the oxidant.[41] Purification was accomplished by three recrystallizations, two from 95% ethanol and a final one from methanol to give white needles, m.p. 102.5-103.2 ^{O}C (lit. m.p. 105 ^{O}C[42]). 3-Methoxyphenanthrene (**2**), was prepared similarly from the photocyclization of 4-methoxystilbene[41] and purified by sublimation at reduced pressure followed by two recrystallizations from 95% ethanol to give white plates, m.p. 57-58 ^{O}C (lit. m.p. 59 ^{O}C[43]). The same samples were used in the X-ray diffraction, the scanning electron microscopy, and the ^{1}H NMR relaxation experiments.

X-ray Diffraction

Crystals of **1** and **2** were mounted on Hampton CryoLoops with Paratone-N and data collected with a Bruker D8 diffractometer using an Ultra rotating-anode generator (Mo) equipped with a high-efficiency multi-layer, double-bounce monochromator.

Experimental details are collected in Table 1. All data were collected with 1.0 sec/1.0^{O} correlated scans. Structure solution and subsequent refinement was routine and used various components of the SHELXTL software package distributed by the Bruker Corporation (G. Sheldrick, Bruker-AXS, Madison WI).

Scanning Electron Microscopy

Field emission scanning electron microscopy[7] was performed on a fee-for-service basis using a FEI Quanta 600FEG Field Emission Scanning Electron Microscope (FESEM) at the Regional Nanotechnology Facility in the Laboratory for Research on the Structure of Matter at the University of Pennsylvania in Philadelphia, Pennsylvania. Images are shown in Figs. 4 and 5. Loose crystalline material from the same samples used with the solid state NMR ^{1}H spin-lattice relaxation experiments was "sprinkled" on graphite conductive adhesive on a cantilevered platform with a 45^{O} slant. By sprinkling the samples on this kind of platform we were able to achieve a variety of orientations for the sample. This wasn't so important for **1** where the crystallites have large somewhat square cross sections but it was particularly important for **2** which was composed of flat thin crystallites. In this case, the random sprinkling potentially allowed for a determination of the smallest crystallite dimension because many crystallites were imbedded on the adhesive in an edge-on orientation. The organic samples are not good electrically conducting materials. To achieve a high resolution image, the specimens must be conductive and well grounded to prevent the accumulation of static electric charge at the surface. Therefore, the samples were thoroughly degassed and then sputtered with approximately 5 nm of gold/palladium (for 20 s at 1 kV and 0.1 mbar) using a Cressington magnetron sputter coater.

NMR Relaxation

^{1}H spin-lattice relaxation experiments were performed at 22.5 and 53.0 MHz in **1** and **2** at temperatures between approximately 110 and 250 K. Temperature control, sensitivity, measurement, and reproducibility is discussed elsewhere.[13] A perturbation π pulse followed by a measure $\pi/2$ pulse sequence was used. The temperature dependence of R, R^*, and R_S in **1** is shown in Fig. 6 and in **2** in Fig. 7 and the temperature dependence of β

in **1** is shown in Fig. 8. R_S is generally difficult to measure accurately[13] because only a short time period of the relaxation curve is being used but it is particularly difficult to determine near the maximum where the departure from exponentiality is slight. At lower temperatures the relaxation is exponential and the single rate R (= R_S) is indicated by the same symbols in Figs. 6 and 7 used for R_S. The uncertainties on R^* and R are taken to be ±6%. This uncertainty is much greater than that returned by the least squares fitting routines and was determined by a numerical exercise adding random noise to exact single and stretched exponential decays. The uncertainties for R_S varied considerably and the uncertainty flags are those returned by the least-squares fitting routine. They are generally larger than ±6%. The scatter in the data at lower temperatures, particularly in **2** can only be due to the presence of slightly different structures on different days since each day's set of experiments can be joined by a single line well within the ±6% uncertainty bars.

Electronic Structure Calculations

Isolated Molecules

All electronic structure calculations were carried out with the Gaussian 09 package of programs.[44] The ground state structures of the isolated molecules of **1** and **2**, were obtained by a geometry optimization at the B3LYP/6-311+G(d,p) level using the X-ray crystallographic structure as a starting point. Potential energy surfaces for the two kinds of rotations were obtained at the B3LYP/6-311+G(d,p)//B3LYP/6-311+G(d,p) level by scanning δ and α (the angles specifying the orientation of the methoxy and methyl groups) from 0^O to 180^O at intervals of 15^O. Additional points were calculated in the vicinity of a stationary point. Calculations were performed with the respective dihedral angle fixed while allowing all other structural parameters to be optimized. The ground state and transition state identified through this scheme are indistinguishable from those obtained directly from locating the minimum and first-degree saddle points. Both ground states and transition states were verified with a normal mode analysis: for ground states, all normal modes have real frequencies whereas transition states have one mode with an imaginary frequency. Barrier heights were taken as the energy difference between the

ground state and transition states and were computed at the B3LYP/6-311+G(d,p)//B3LYP/6-311+G(d,p) level.

Clusters

Cluster models of **1** and **2** were constructed from the single-crystal X-ray structures to mimic the intermolecular environment in the crystals. A 10-molecule cluster and a 14-molecule cluster (Fig. 2) of **1** were constructed to examine the cluster size effect to the calculated barriers. Only one cluster consisting of 12 molecules was built for **2** (Fig. 3). The environment of the central molecule in each cluster simulates the crystal packing interactions as experienced by a molecule in an ideal crystal. By fixing all C and O atoms at their positions as determined in the X-ray structure, the positions of H atoms were determined by a partial geometry optimization at the B3LYP/6-31G(d) level. Prior experience[2, 3, 11, 12, 28, 40] shows that the 10-molecule cluster for **1** and the 12-molecule cluster for **2** are large enough that all neighboring molecules with significant intermolecular interactions with the central molecule have been included. Adding more neighboring molecules would not significantly change the calculated barriers. However, we also performed calculations with a 14-molecule cluster of **1** and, as reported in the Results section, the results are essentially the same as the 10-molecule cluster.

Potential energy surfaces (PESs) were calculated for the internal rotations (methyl and methoxy groups) on the central molecule of each cluster. Two groups of calculations were performed. In the *rigid rotation model,* only the angle δ (methoxy group angle) or α (methyl group angle) on the target molecule (see Figs 2 and 3) in the cluster was changed and calculations were done for 15^{O} steps in δ and α with additional points around the ground state and the transition state in this rigid potential energy surface. The rotational ground and transition states of the methyl group identified from these calculations were subject to additional partial relaxation calculations. In **1**, four stages of *partial relaxation* were applied in sequential order to include more and more degrees of structural relaxational freedom. In *stage one* of the *partial relaxation model*, only the structural parameters of the methoxy group and the H atoms on the target molecule were allowed to relax. In *stage two*, the two dihedral angles δ and α in all the other molecules in the cluster were also allowed to relax. In *stage three*, all the

structural parameters of the methoxy groups and hydrogen atoms in the clusters were allowed to relax. In *stage four*, the phenanthrene carbons on the home molecule were also allowed to relax. During each stage, three calculations were done in parallel, one for the transition state and two for the ground state. For the two calculations for the ground state, the difference lies in whether the corresponding rotational coordinate is fixed at the value found in the rigid rotation model or not. In all cases, we obtained the same results for the two ground state calculations and this provides additional confidence in our computational approach. Comparing the results for these four stages provides insight to the origin of the dominant interactions responsible for the methyl group barriers.

Following this thorough investigation with **1**, we did a simpler set of calculations for **2** since the conclusion obtained in the studies of **1** should be applicable to **2**. For **2**, a two-stage *partial relaxation model* was performed. The first stage was the same as *stage one* for **1** in which only the structural parameters of the methoxy group and all the H atoms on the home molecule were allowed to relax. The other stage corresponds to *stage three* for **1** in which the structural parameters of all the methoxy groups and H atoms in the cluster, not just those on the target molecule, were allowed to relax.

Rotational barriers were taken to be the difference in the calculated energies between the ground and transition states for methyl group rotation and for methoxy group rotation. Previous studies have shown that the barriers obtained from the partial relaxation models are comparable with the rotational activation energy as measured by solid-state NMR relaxation experiments.[2, 3, 11, 12, 28, 40]

References

[1] K. G. Conn, P. A. Beckmann, C. W. Mallory, F. B. Mallory, *J. Chem. Phys*. **1987**, *87*, 20-27.

[2] P. A. Beckmann, K. G. Conn, C. W. Mallory, F. B. Mallory, A. L. Rheingold, L. Rotkina, X. Wang, *J. Chem. Phys*. **2013**, *139*, 204501, 1-12.

[3] X. Wang, P. A. Beckmann, C. W. Mallory, A. L. Rheingold, A. G. DiPasquale, P. J. Carroll, F. B. Mallory, *J. Org. Chem.* **2011**, *76*, 5170-5176.

[4] S. Clough, A. Heidemann, *J. Phys. C* **1980**, *13*, 3585-3589.

[5] R. Kimmich, *NMR Tomography, Diffusometry, Relaxometry* (Springer-Verlag: Berlin, 1997).

[6] R. Tilley, *Crystals and Crystal Structures* (Wiley, Chichester, UK, 2006).

[7] J. Goldstein, D. E. Newbury, D. C. Joy, C. E. Lyman, P. Echlin, E. Lifshin, L. Sawyer, J. R. Michael, *Scanning Electron Microscopy and X-ray Microanalysis, 3rd ed.*, (Springer Science + Business Media, New York, 2003).

[8] J. Kohanoff, *Electronic Structure Calculations for Solids and Molecules: Theory and Computational Methods* (Cambridge Univ. Press, Cambridge, UK, 2006).

[9] J. Kowalewski, T. Liljefors, *Chem. Phys. Lett*. **1979**, *64*, 170-174.

[10] O. Edholm, C. Blomberg, *Chem. Phys*. **1981**, *56*, 9-14.

[11] D. P. Fahey, W. G. Dougherty Jr., W. S. Kassel, X. Wang, P. A. Beckmann, *J. Phys. Chem. A* **2012**, *116*, 11946-11956.

[12] X. Wang, L. Rotkina, H. Su, P. A. Beckmann, *ChemPhysChem* **2012**, *13*, 2082-2089.

[13] P. A. Beckmann, E. Schneider, *J. Chem. Phys.* **2012**, *136*, 054508, 1-9.

[14] X. Jiang, B. Rodríguez-Molina, N. Nazarian, M. A. Garcia-Garibay, *J. Am. Chem. Soc.* **2014**, *136*, 8871–8874.

[15] P. Commins, Miguel A. Garcia-Garibay, J*. Org. Chem.* **2014**, *79*, 1611–1619.

[16] L. Kobr, K. Zhao, Y. Shen, R. K. Shoemaker, C. T. Rogers, J. Michl, *Crystal Growth & Design* **2014**, *14*, 559–568.

[17] B. Rodríguez-Molina, S. Pérez-Estrada, M. A. Garcia-Garibay, *J. Am. Chem. Soc.* **2013**, *135*, 10388–10395.

[18] E. Escalante-Sánchez, B. Rodríguez-Molina, M. A. Garcia-Garibay, *J. Org. Chem.* **2012**, *77*, 7428–7434.

[19] Z. J. O'Brien, A. Natarajan, S. Khan, M. A. Garcia-Garibay, *Crystal Growth & Design* **2011**, *11*, 2654–2659.

[20] A. S. Lubbe, N. Ruangsupapichat, G. Caroli, B. L. Feringa. *J. Org. Chem.* **2011**, *76*, 8599–8610.

[21] M. A. Garcia-Garibay, C. E. Godinez, *Crystal Growth & Design* **2009**, *9*, 3124–3128.

[22] A. Abragam, *The Principles of Nuclear Magnetism* (Oxford Univ. Press, Oxford, 1961).

[23] R. L. Hilt, P. S. Hubbard, *Phys. Rev.* **1964**, *134*, A392-A398.

[24] L. K. Runnels, *Phys. Rev*. **1964**, *134*, A28-A36.

[25] N. L. Owen, in *Internal Rotation in Molecules*, ed. W. J. Orville-Thomas (Wiley, New York, 1974), p. 157.

[26] D. W. Davidson, R. H. Cole, *J. Chem. Phys.* **1951**, *19*, 1484-1421.

[27] P. A. Beckmann, *Phys. Rep.* **1988**, *171*, 85-128.

[28] X. Wang, F. B. Mallory, C. W. Mallory, H. R. Odhner, P. A. Beckmann, *J. Chem. Phys*. **2014**, *140*, 194304, 1-15.

[29] V. L. Deringer, V. Hoepfner, R. Dronskowski, *Cryst. Growth & Design* **2012**, *12*, 1014-1021.

[30] T. Steiner, W. Saenger, *Acta Cryst. A* **1993**, *49*, 379-384.

[31] A. D. Becke, *J. Chem. Phys.* **1993**, *98*, 5648-5652.

[32] C. Lee, W. Yang, R. G. Parr, *Phys. Rev. B* **1988**, *37*, 785-789.

[33] S. H. Vosko, L. Wilk, M. Nusair, *Can. J. Phys.* **1980**, *58*, 1200-1211.

[34] L. M. Mentel, E. J. Baerends, *J. Chem. Theory Comput.* **2014**, *10*, 252-267.

[35] S. Simon, M. Duran, J. J. Dannenberg, *J. Chem. Phys.* **1996**, *105*, 11024-11031.

[36] H. Kruse, S. Grimme, *J. Chem. Phys.* **2012**, *136*, 154101, 1-16.

[37] S. Grimme, *WIREs Comp. Mol. Sci.* **2011**, *1*, 211–228,

[38] V. N. Staroverov, G. E. Scuseria, J. Tao, J. P. Perdew, *J. Chem. Phys*. **2003**, *119*, 12129-12137.

[39] Y. Zao, D. G. Truhlar, *Theor. Chem. Account* **2008**, *120*, 215-241.

[40] X. Wang, F. B. Mallory, C. W. Mallory, P. A. Beckmann, A. L. Rheingold, M. M. Francl, *J. Phys. Chem. A* **2006**, *110*, 3954-3960.

[41] C. S. Wood, F. B. Mallory, *J. Org. Chem*. **1964**, *29*, 3373-3377.

[42] L. F. Fieser, *J. Am. Chem. Soc*. **1929**, *51*, 2460-2469.

[43] R. Pschorr, *Berichte der Deutschen Chemischen Gesellschaft* **1901**, *34*, 3998-4007.

[44] Gaussian 09, Revision D.01, M. J. Frisch, G. W. Trucks, H. B. Schlegel, G. E. Scuseria, M. A. Robb, J. R. Cheeseman, G. Scalmani, V. Barone, B. Mennucci, G. A. Petersson, H. Nakatsuji, M. Caricato, X. Li, H. P. Hratchian, A. F. Izmaylov, J. Bloino, G. Zheng, J. L. Sonnenberg, M. Hada, M. Ehara, K. Toyota, R. Fukuda, J. Hasegawa, M. Ishida, T. Nakajima, Y. Honda, O. Kitao, H. Nakai, T. Vreven, J. A. Montgomery, Jr., J. E. Peralta, F. Ogliaro, M. Bearpark, J. J. Heyd, E. Brothers, K. N. Kudin, V. N. Staroverov, R. Kobayashi, J. Normand, K. Raghavachari, A. Rendell, J. C. Burant, S. S. Iyengar, J. Tomasi, M. Cossi, N. Rega, J. M. Millam, M. Klene, J. E. Knox, J. B. Cross, V. Bakken, C. Adamo, J. Jaramillo, R. Gomperts, R. E. Stratmann, O. Yazyev, A. J. Austin, R. Cammi, C. Pomelli, J. W. Ochterski, R. L. Martin, K. Morokuma, V. G. Zakrzewski, G. A. Voth, P. Salvador, J. J. Dannenberg, S. Dapprich, A. D. Daniels, Ö. Farkas, J. B. Foresman, J. V. Ortiz, J. Cioslowski, D. J. Fox, Gaussian, Inc., Wallingford CT, 2009.

Table 1. Crystallographic Data. See Table 2 and Fig. 1 for the names.

Compound	**1**	**2**	**3**	**4 (100 K)**	**4 (200 K)**
Empirical Formula	$C_{15}H_{12}O$	$C_{15}H_{12}O$	$C_{14}H_{14}O_2$	$C_{14}H_6F_8O_2$	$C_{14}H_6F_8O_2$
Formula Weight	208.25	208.25	214.26	358.19	358.19
Temp (K)	100	100	113	100	200
Wavelength (Å)	0.71073	0.71073	0.71073	1.54178	1.54178
Crystal System	tetragonal	orthorhombic	orthorhombic	orthorhombic	orthorhombic
Space Group	*I*-4	$P2_12_12_1$	*Pbca*	*Pbcn*	*Pbcn*
a (Å)	18.2516(8)	5.6515(5)	7.2869(6)	13.1644(4)	13.1708(5)
b (Å)		10.1528(10)	6.1450(6)	7.7256(3)	7.8476(2)
c (Å)	6.4046(4)	18.4646(18)	24.622(3)	12.5307(5)	12.6056(4)
V (Å^3)	2133.51(9)	1059.47(17)	1102.524(2)	1247.41(9)	1302.90(7)
Z	8	4	4	4	4
Z' (# molecules)	1	1	1/2	1/2	1/2
Rflns (collect/indepnt)	4355/1507	8441/1932	-	4613/1115	3645/1128
*R*1/*wR2* (2σ(I))	3.46/7.58	3.54/8.10	-	3.09/9.40	4.91/13.29
GOF	0.982	0.998	-	1.070	1.085
reference	this work	this work	reference 12	reference 11	reference 11
CCDC[a] reference			JEHDEG	WOQFAL01	WOQFALW

[a]Cambridge Crystallographic Data Centre <http://www.ccdc.cam.ac.uk>

Table 2. Parameters characterizing methyl group and methoxy group rotation.

		OCH_3	CH_3	OCH_3	OCH_3	CH_3	CH_3	OCH_3	ref
		V_{iso}	V_{iso}	rotation	V_{clust}	NMR *E*	V_{clust}	rotation	
		kJ mol^{-1}	kJ mol^{-1}	from/to	kJ mol^{-1}	kJ mol^{-1}	kJ mol^{-1}	from/to	
				iso molec[a]				crystal[b]	
1	1-methoxyphenanthrene	40.5	13.8	0^O to 30^O	>800	16(2)	16.6	5^O to10^O	this work
2	3-methoxyphenanthrene	13.7	13.8	0^O to 27^O	>800	16(2)	13.4	9^O to16^O	this work
3	4,4'-dimethoxybiphenyl	12.3	12.8	0^O to 30^O	>2000	11.5(5)	10.3	3^O to19^O	12, 13
4	4,4'-dimethoxyoctafluorobiphenyl	1.3	4.1	40^O to 57^O	>300	17(2)	17.1	13^O to 42^O	11

[a]OCH_3 rotation when CH_3 rotates from the ground state to the transition state in the isolated molecule
[b]OCH_3 rotation when CH_3 rotates from the ground state to the transition state in the cluster

Table 3. Rotational barriers (in kJ mol^{-1}) of methyl groups in the clusters of 1-methoxyphenanthrene (**1**) and 3-methoxyphenanthrene (**2**).

	Size[a]	Rigid[b]	Partially Relaxed[c]				
		B3LYP	B3LYP[d]	BSSE[d,e]	D3BJ[d,f]	TPSSh[g]	M06-2X[g]
1	10	25.5	16.2	15.4	16.8	16.1	19.3
	14	25.2	16.6[h]	15.6	17.2	16.4	20.0
2	12	25.2	13.4[h]				

[a]number of molecules in the cluster
[b]Rigid rotation model;
[c]Partially relaxed rotation model;
[d]Calculated at the B3LYP/6-31G(d) level;
[e]With the basis set superposition error corrected;
[f]With the Grimme's D3BJ correction for the London's dispersion;
[g]Calculated with the 6-31G(d) basis set.
[h]Final values reproduced in Table 2 as V_{clust}

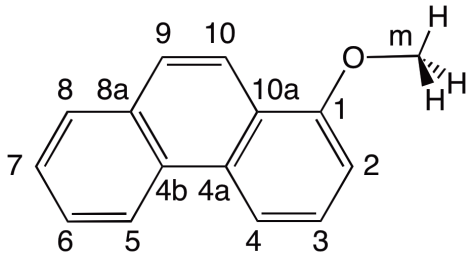

1-methoxyphenanthrene (**1**)

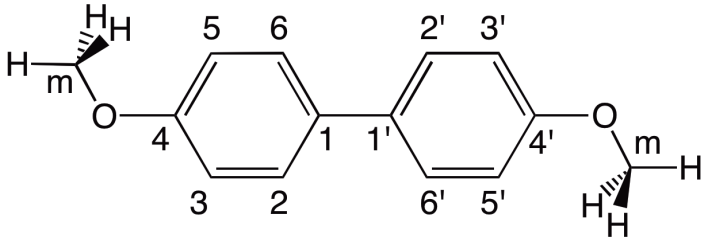

4,4'-dimethoxybiphenyl (**3**)

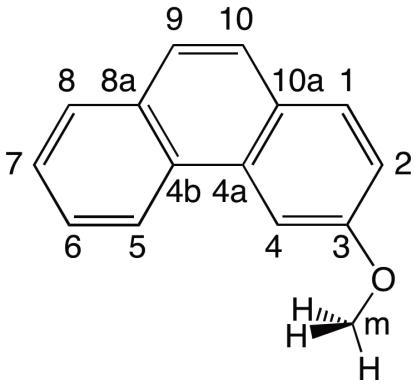

3-methoxyphenanthrene (**2**)

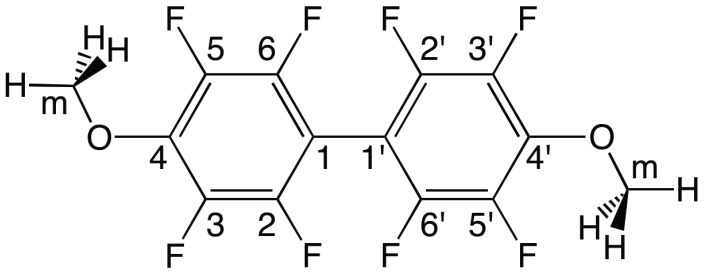

4,4'-dimethoxyoctafluorobiphenyl (**4**)

Fig. 1. Schematic pictures of 1-methoxyphenanthrene (**1**), 3-methoxyphenanthrene (**2**), 4,4'-dimethoxybiphenyl (**3**), and 4,4'-dimethoxyoctafluorobiphenyl (**4**), all showing the methoxy groups in their ground state in the isolated molecules.

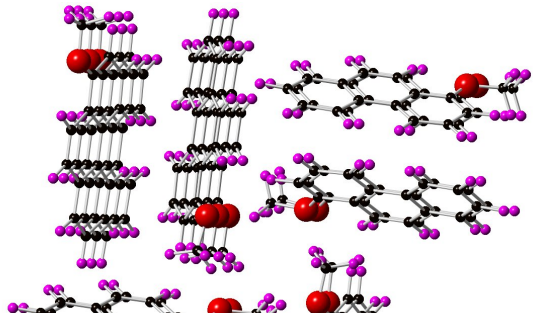

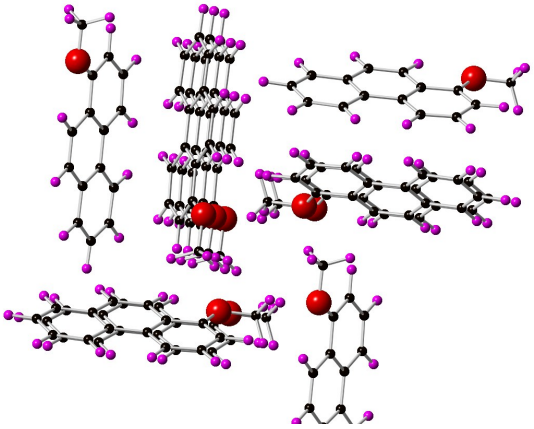

(a)

(b)

Fig. 2. (Colour on line.) **(a)** the 10-molecule and **(b)** 14-molecule clusters of 1-methoxyphenanthrene (**1**). Carbon atoms are small black spheres, hydrogen atoms are small purple spheres, and oxygen atoms are large red spheres. The view is one obtained by a rotation of a few degrees around the (vertical) *y*-axis from the 010 plane where the nearly superimposed molecules would be exactly superimposed. The target methoxy group for the electronic structure calculations is the central one of the three nearly superimposed methoxy groups in both (a) and (b).

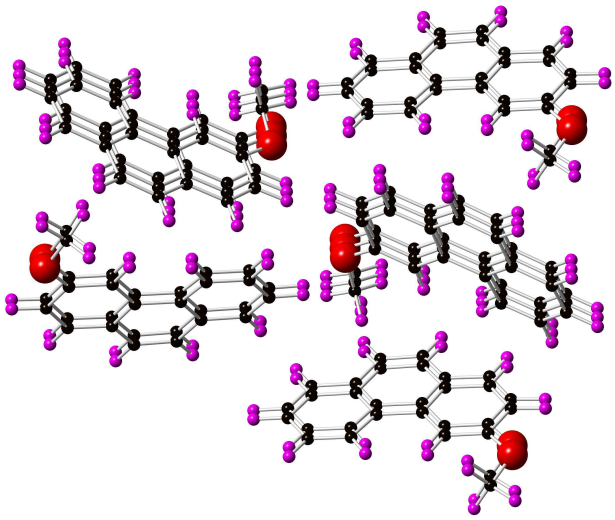

Fig. 3. (Colour on line.) The 12-molecule cluster of 3-methoxyphenanthrene (**2**). Carbon atoms are small black spheres, hydrogen atoms are small purple spheres, and oxygen atoms are large red spheres. The view is one obtained by a rotation of a few degrees around the (horizontal) z-axis from the 100 plane where the nearly superimposed molecules would be exactly superimposed. The target methoxy group for the electronic structure calculations is the central one of three nearly superimposed methoxy groups.

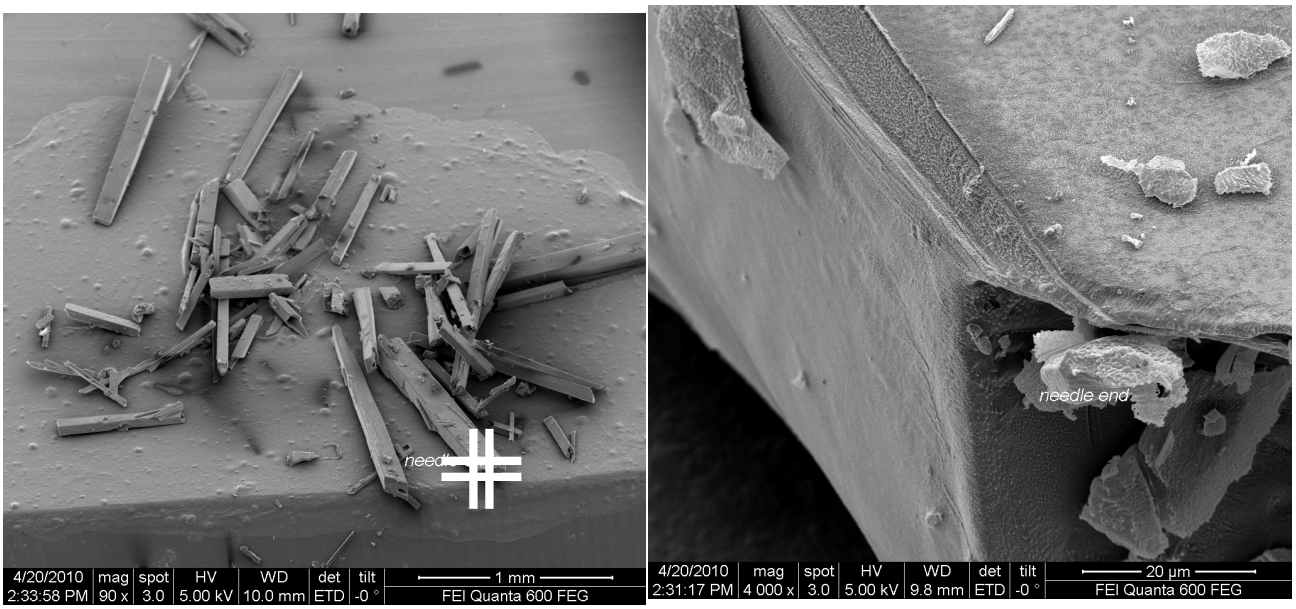

(a) **(b)**

Fig. 4. Field emission scanning electron microscopy images of 1-methoxyphenanthrene (**1**). **(a)** The entire SEM sample; 3.2 X 2.9 mm. **(b)** A 73 X 64 μm image showing the region in the box in (a). The large majority of crystallites have a smallest dimension of 15 – 40 μm.

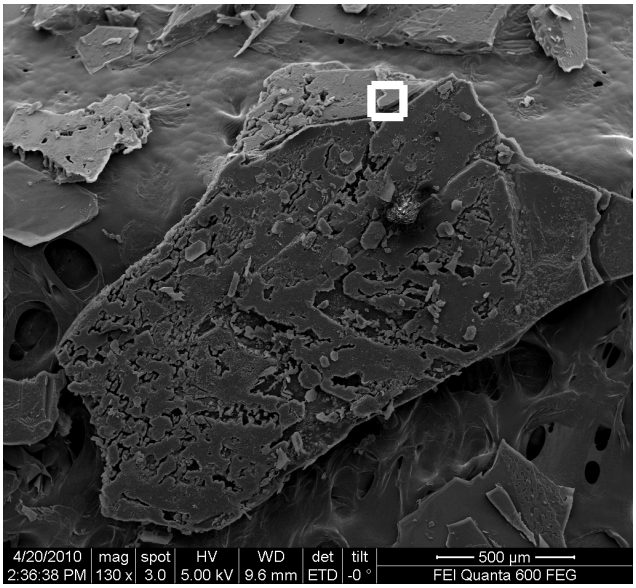

(a)

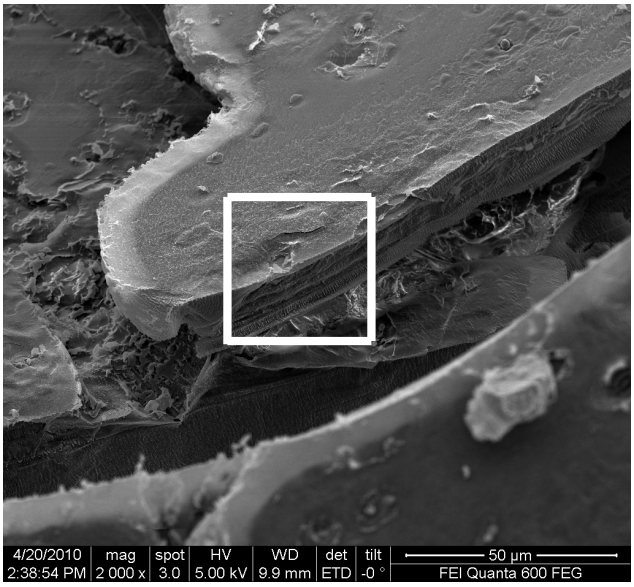

(b)

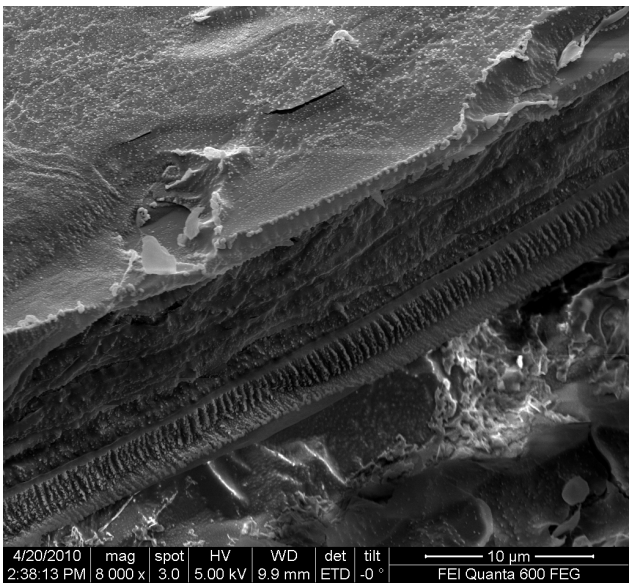

(c)

Fig. 5. Field emission scanning electron microscopy images of 3-methoxyphenanthrene (**2**). **(a)** A 2.2 X 2.0 mm part of the sample. **(b)** A 150 X 130 μm image showing the region in the box in (a) The image in (a) suggests that this a break in the large crystallite. **(c)** A 37 X 32 μm image showing the region of the break in the box in (b). The large majority of crystallites have this smallest dimension of 5 – 10 μm but, as discussed in the text, this may be hundreds of stacked very thin crystallites.

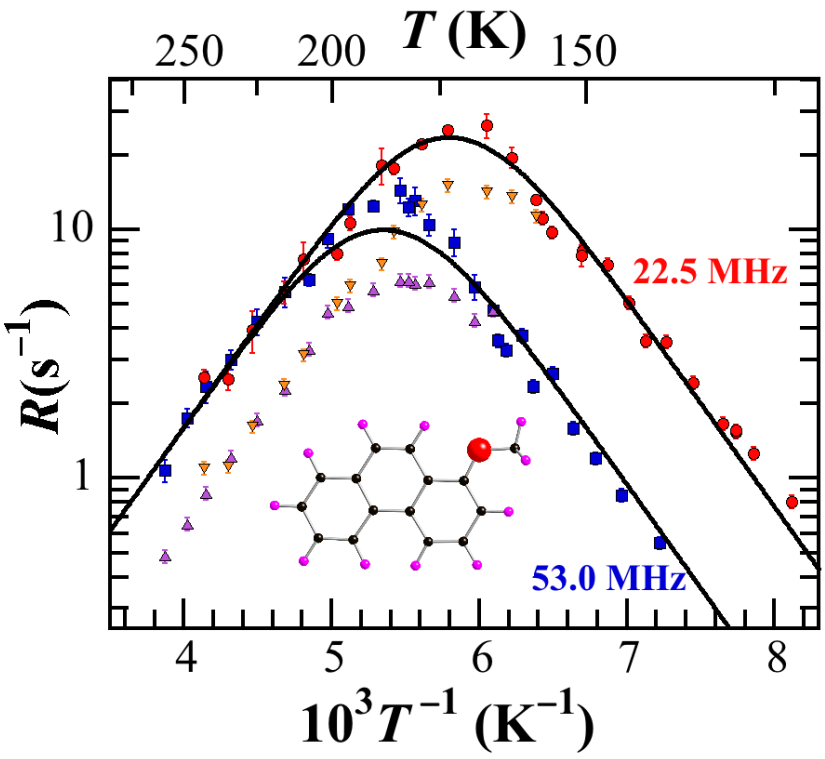

Fig. 6. (Colour on line.) Solid state ^{1}H spin-lattice relaxation rates versus inverse temperature T^{-1} in 1-methoxyphenanthrene (**1**) at 22.5 MHz [R and R_S (●), R^* (▼)] and 53.0 MHz [R and R_S (■), R^* (▲)]. The fit is a single Poisson model fit to R and R_S. The R^* values play no role in the fitting procedure.

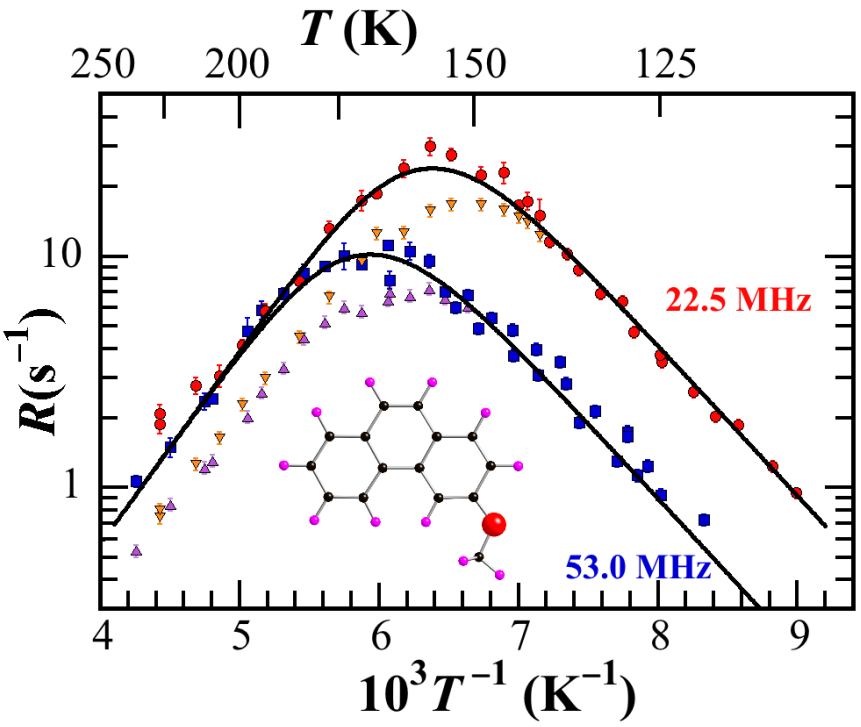

Fig. 7. (Colour on line.) ^{1}H spin-lattice relaxation rates versus inverse temperature T^{-1} in 3-methoxyphenanthrene (**2**) at 22.5 MHz [R and R_S (●), R^* (▼)] and 53.0 MHz [R and R_S (■), R^* (▲)]. The fit is a Davidson-Cole fit to R and R_S. The R^* values play no role in the fitting procedure.

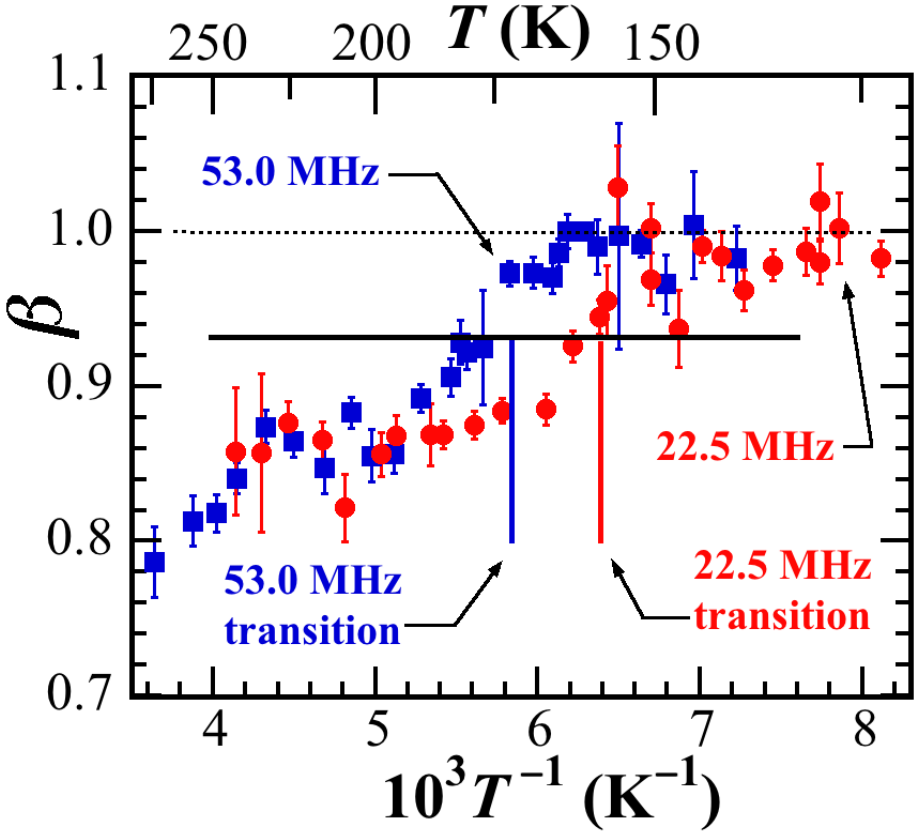

Fig. 8. (Colour on line.) The stretching parameter β versus inverse temperature T^{-1} for 1-methoxyphenanthrene (**1**) at 22.5 MHz (●) and 53.0 MHz (■). The horizontal full line is drawn at $\beta = 0.93$ and marks the approximate distinction between exponential ($\beta > 0.93$) and nonexponential ($\beta < 0.93$) relaxation. This occurs approximately at the temperatures indicated by the vertical lines for the two NMR frequencies. The dotted horizontal line indicates $\beta = 1$.

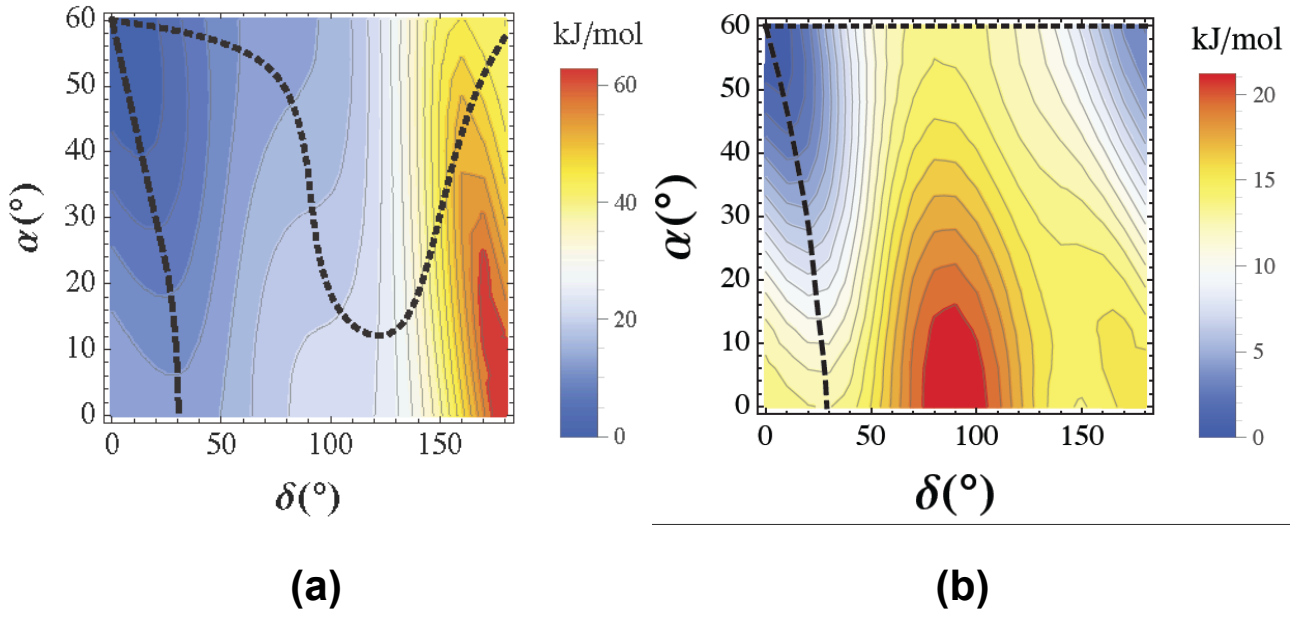

Fig. 9. (Colour on line) The energy of an isolated molecule of **(a)** 1-methoxyphenanthrene (**1**) and **(b)** 3-methoxyphenanthrene (**2**) calculated at the B3LYP/6-311+G(d,p)//B3LYP/6-311+G(d,p) level as a function methoxy group rotation angle δ and methyl group rotation angle α. The ground state (δ, α) = (0^{O}, 60^{O}) is taken as the zero of energy. The contour lines are lines of constant energy and the lines are separated by approximately 3 kJ $mole^{-1}$ in (a) and by approximately 1 kJ $mole^{-1}$ in (b). The short dashed lines show the coupled rotation as the methoxy group rotates from its ground state to its transition state and the long dashed lines show the coupled rotation as the methyl group rotates from its ground state to its transition state.

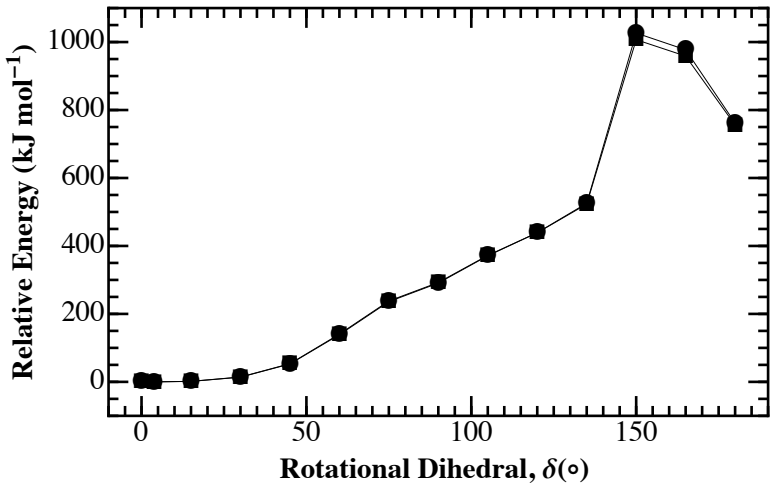

Fig. 10. The potential energy surface (PES) for methoxy group rotation for a methoxy group at the center of clusters of 1-methoxyphenanthrene (**1**) (●) and 3-methoxyphenanthrene (**2**) (■) calculated with the *rigid rotation model*. The angle δ is the rotational dihedral angle Cm-O-C1-C2 in **1** and Cm-O-C3-C4 in **2** (see Fig. 1) where Cm is a methyl carbon atom. At the resolution shown, the two curves are essentially indistinguishable.

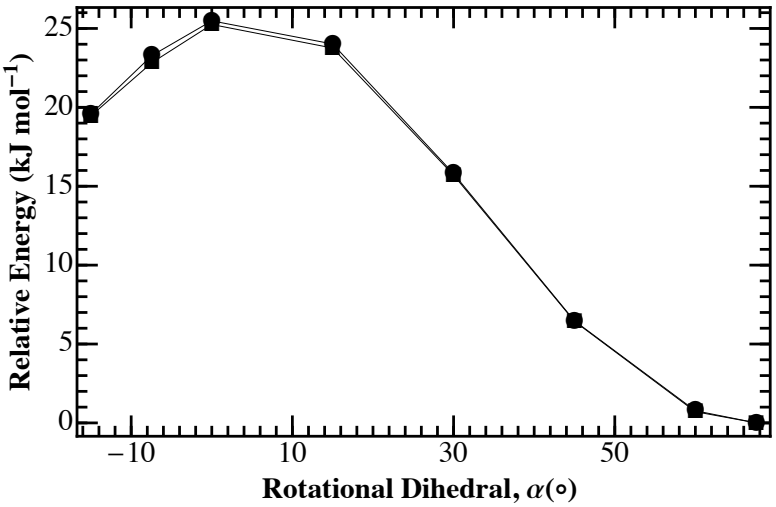

Fig. 11. The potential energy surface (PES) for methyl group rotation for a methyl group on the target molecule at the center of clusters of 1-methoxyphenanthrene (**1**) (●) and 3-methoxyphenanthrene (**2**) (■) calculated with the *rigid rotation model*. The angle α is the rotational dihedral angle H-Cm-O-C1 in **1** and H-Cm-O-C3 in **2** (see Fig. 1) where Cm is a methyl carbon atom. At the resolution shown, the two curves are essentially indistinguishable.